



Differences in Pilon Fractures According to Ipsilateral Fibular Injury Patterns: A Clinical Computed Tomography-Based Mapping Study

Jae-Hwan Lim, MD, Jun-Young Lee, MD*, Ba-Rom Kim, MD*, Suenghwan Jo, MD*,
Dong-Hyuk Cha, MD*, Hyo-Jun Lee, MD*, Gu-Hee Jung, MD^{†,‡}

Department of Orthopedic Surgery, Gwangju Suwan Hospital, Gwangju,

**Department of Orthopedic Surgery, Chosun University Hospital, Chosun University College of Medicine, Gwangju,*

*†Department of Orthopedic Surgery, Gyeongsang National University Changwon Hospital,
Gyeongsang National University College of Medicine, Changwon,*

‡Medical ICT Convergence Research Center, Institute of Health Sciences, Gyeongsang National University College of Medicine, Jinju, Korea

Background: Preoperative verification of fracture morphology is essential for determining the definitive fixation strategy in the management of a pilon fracture. This study aimed to determine the correlation between fibular injury patterns and fracture morphologies and introduce clinical implications.

Methods: Computed tomography scans of 96 pilon fractures were retrospectively analyzed and divided into three types: intact fibula, simple fracture, and multifragment fracture. The principal fracture line and comminution zones were illustrated on a plafond template and diagrammatized on a 6 × 6 grid using PowerPoint software as fracture mapping. Correlations between fibular injury patterns and fracture morphologies, including comminution zones and principal fracture lines, were analyzed.

Results: The thickest comminution zone was most often located in the anterolateral quadrant. According to fibular injury patterns, the comminution zone of the multifragment group was placed two grids more lateral than that of other groups. Lateral exits of the principal fracture line in the multifragment group were much more concentrated within the fibular incisura.

Conclusions: In pilon fractures, a more complex fibular fracture pattern was related to the valgus position. Moreover, the articular fracture pattern of pilon fractures differed according to coronal angulation and fibular fracture pattern. These differences should influence the operative approach and placement of the plate.

Keywords: *Fibular, Ankle joint, Pilon Fracture, Fracture pattern, Fracture mapping*

Although the trend of management of complex pilon fractures has been changed toward staged protocols of temporary external fixation, the main goal is to restore and fix

the articular surface, as well as the geometric integrity of ankle joint, sufficiently to allow early joint motion.¹⁾ With the implementation of a staged surgical treatment protocol

Received June 8, 2022; Revised October 5, 2022; Accepted November 8, 2022

Correspondence to: Jun-Young Lee, MD

Department of Orthopedic Surgery, Chosun University Hospital, 365 Pilmun-daero, Dong-gu, Gwangju 61453, Korea

Tel: +82-62-220-3147, Fax: +82-62-226-3379, E-mail: leejy88@chosun.ac.kr

Co-Correspondence to: Gu-Hee Jung, MD

Department of Orthopedic Surgery, Gyeongsang National University Changwon Hospital, Gyeongsang National University College of Medicine, 11 Samjeongja-ro, Seongsan-gu, Changwon 51472, Korea

Tel: +82-55-214-3822, Fax: +82-55-214-3259, E-mail: jyujin2001@hotmail.com

Copyright © 2023 by The Korean Orthopaedic Association

This is an Open Access article distributed under the terms of the Creative Commons Attribution Non-Commercial License (<http://creativecommons.org/licenses/by-nc/4.0>) which permits unrestricted non-commercial use, distribution, and reproduction in any medium, provided the original work is properly cited.

Clinics in Orthopedic Surgery • pISSN 2005-291X eISSN 2005-4408

along with the evolution of implant technology, complication rates have decreased while clinical and functional outcomes have been improved.²⁾ However, Penny et al.³⁾ have noted that none of the available plates could substitute for an understanding of fracture planes or fragments that are typically seen in complex pilon fractures. Thus, the surgeon should determine a preoperative strategy involving an optimal approach and definitive fixation based on the severity of the articular surface injury and metaphyseal comminution.⁴⁾

Concerning the ipsilateral fibular injury in the management of pilon fractures, the assessment of patterns and locations is critical, especially for restoring the original length and rotation.⁵⁻⁷⁾ Ipsilateral fibular injury patterns have been used as an indicator of the application mode of the impaction force by discriminating the tension (varus force) and compression failure (valgus force).¹⁾ Clinically, ipsilateral fibular fractures exist not only as comminuted and transverse fractures, but also as oblique fractures and spiral fractures. Additionally, there are no scientific data to prove that the fracture pattern can be used to determine whether the mode of fibular failure is compression or tension. Several studies^{5,8,9)} have been abstractly conducted under the premise that comminuted fibular fractures occur as a result of valgus stress, whereas transverse fractures of the fibula reveal varus angulation.

Therefore, the objectives of this study were as follows: (1) to determine fracture characteristics with mapping using three-dimensional (3D) biplanar images of computed tomography (CT), (2) to identify differences of principal fracture lines and comminution zones according to fibular injury patterns, and (3) to assess the usefulness of fibular injury patterns as a preoperative indicator to de-

termine optimal approaches and fixation strategies.

METHODS

This study retrospectively analyzed medical records and radiographs of distal tibial fractures after obtaining approval from the Ethics Committee of Chosun University College of Medicine (No. CHOSUN 2020-03-026). In addition, the requirement for informed consent was waived. By reviewing radiographs, which were taken at the time of injury, 145 patients were diagnosed with a distal tibial intra-articular fracture at our institution between August 2008 and March 2019. Among them, patients with an ipsilateral talus fracture and ankle joint deformity from the previous operation and trauma, patients younger than 18 years of age, and patients aged 75 years or older were excluded. Two board-certified orthopedic surgeons who had completed the fellowship in foot and ankle surgery (JHL and DHC) reviewed whether included patients met the definition of pilon fractures by reviewing injury history and radiographic findings including CT scanning images. Thirty-three patients in whom fractures were not caused by axial impaction (high-energy injury) were excluded. Finally, 96 patients (79 men and 17 women) were enrolled in this study. Of these, 56 patients underwent CT without spanning external fixators, and 40 patients, after spanning external fixators. The average age of the patients was 47

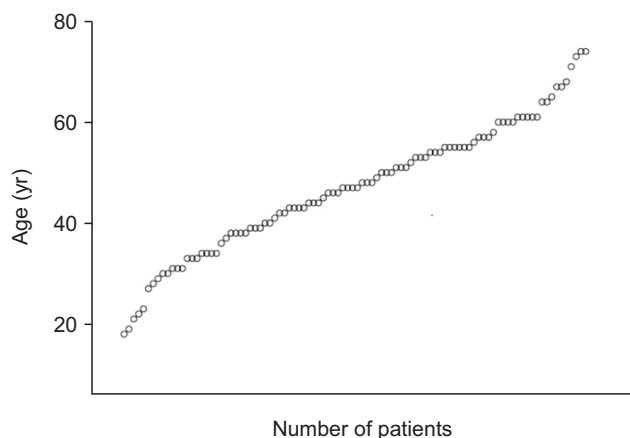


Fig. 1. The age distribution of the study population was uniform so that the results were not compromised by a specific weight distribution for age or bone quality.

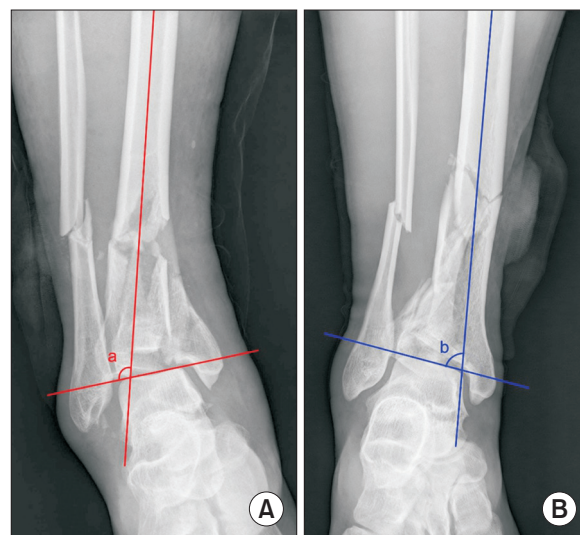


Fig. 2. Anteroposterior radiographs of pilon fractures before intervention. Not all comminuted fibular fractures show valgus angulation. Not all transverse fibular fractures show varus angulation. (A) Radiograph showing varus angulation in a multifragment fibular fracture. a: lateral tibiotalar angle (LTTA) is 106.38°. (B) Radiograph showing valgus angulation in a simple fibular fracture. b: LTTA is 78.13°.

years (range, 18–74 years; standard deviation [SD], 13.4) with uniform age distribution (Fig. 1). Among 23 (24%) cases of open fractures, there was 1 case (4.3%) of type I based on the Gustilo and Anderson classification,¹⁰ 21 cases (91.3%) of type IIIA, and 1 case (4.3%) of type IIIB fracture. Mechanisms of injury were falls in 72 cases (75%), motor vehicle accidents in 21 cases (21.9%), and slipping in 3 cases (3.1%).

All measurements of this study were performed by using tools of Picture-Archiving Communications System (GE). To confirm the proximal fibula fracture, the full-length radiograph of the tibia was checked. Ipsilateral fibular injury patterns of the enrolled cases were divided into intact fibula (no fracture), simple fracture (two fragments of any fracture type: transverse, oblique, and spiral), and multifragment fracture (three fragments or more: segmental, wedge, and comminuted). Based on lateral tibiotalar angle (LTTA) of 89° using initial anteroposterior radiographs of the ankle on the assumption of the absence of talar tilt,¹¹ pilon fractures were classified into varus and valgus groups (Fig. 2). Through analysis of CT scanning images, pilon fractures were categorized using the Rüedi-Allgöwer classification,¹² the simplified AO/Orthopaedic Trauma Association (OTA) classification (type B of partial articular fracture and type C of complete articular fracture),¹³ and the Topliss classification (coronal and sagittal family).¹⁴ All fractures were reviewed twice by a fellowship-trained trauma surgeon (GHJ) and two senior

orthopedic residents (BRK and HJL). If there was a difference even after four attempts of classification, the senior surgeon (JYL) decided on the final classification.

To create a template for tibial plafond (plafond template), 10 patients who underwent CT scanning for reasons other than fracture/deformity were used. Their average age was 46.3 years (range, 27–66 years; SD, 12.0). For the plafond template, the 3D biplanar image of CT scanning was obtained after subtracting the tarsal bone of the talus and calcaneus. The true cephalad view of the plafond was used. Plafond templates were diagrammatized on a 6 × 6 grid by connecting border lines of each grid in PowerPoint software (Microsoft) (Fig. 3). For fragments with displacement, the location of the fracture line was estimated by imagining that the fragment was virtually reduced and diagrammatized within the 6 × 6 grids. Principal and other fracture lines are illustrated in different colors (pilon map) by modifying the method described by Cole et al.¹⁵ and McGonagle et al.¹⁶ Tiny fragments less than 10 mm were not diagrammatized or incorporated in the comminution zone (Fig. 3). Regarding three maps independently illustrated by a trauma surgeon (GHJ) and two senior orthopedic residents (BRK and HJL), definitive positions of the principal fracture line and comminution zone were fine-tuned and verified definitively by the corresponding author (JYL). Maps of each group (intact fibula, simple, and multifragment fracture groups) were superimposed using Photoshop CC software (Adobe Sys-

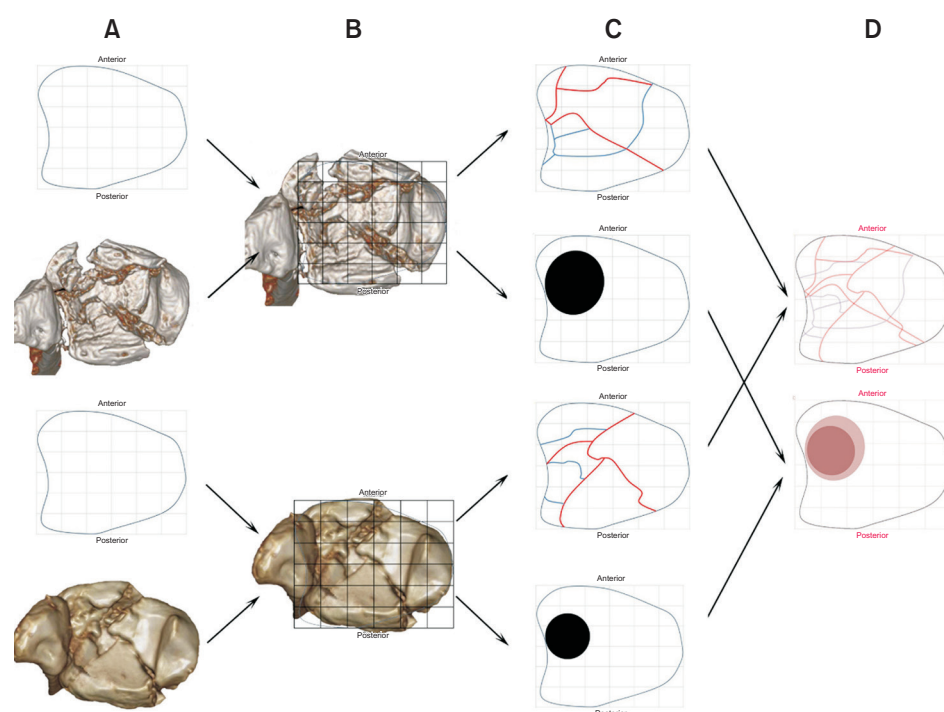


Fig. 3. Mapping method for presenting the fracture line and comminution zone. (A) Standardized template and a three-dimensional reconstructed image produced with the Aquarius program. (B) Overlapping of two images. (C) Imagined and illustrated virtual reduction. Diagrammatized fracture lines and comminution sites shown on the template. The red line represents the main fracture line. The blue line represents the secondary fracture line. The black circle represents the comminution zone. (D) Superimposed images of fracture lines and comminution zones.

tems). Afterwards, comparison of fracture lines and continuation zones was carried out.

The intraclass correlation coefficient was used to determine inter- and intraobserver reliability. The correlation of pilon map was analyzed according to radiological findings, including fibular injury patterns, varus/valgus angulation, and fracture classification. All statistical analyses were performed using IBM SPSS ver. 20 (IBM Corp.). A value of $p < 0.05$ was considered statistically significant. A linear-by-linear association test was performed to compare the ratio of varus or valgus position between the three fibular fracture pattern groups (intact, simple, and multi-

fragment). Moreover, we performed a one-way analysis of variance test to compare the difference in the mean LTТА among the three fibular fracture pattern groups, followed by Dunnett's T3 pairwise comparison post hoc test to determine significant differences between individual groups. Pearson's chi-square test and Fisher's exact test were performed to confirm the correlation between the fibular fracture pattern and coronal angulation of the pilon fractures.

RESULTS

All patient characteristics are summarized in Table 1.

Table 1. Overall Characteristics and Comparison of Pilon Fracture Based on Fibular Fracture Pattern

Variable	Total (n = 96)	Intact fibular (n = 33)	Simple fracture (n = 33)	Multi-fragment fracture (n = 30)	p-value
Age (yr)	47.0 ± 12.97 (18–74)	41.3 ± 12.15 (18–68)	48.3 ± 11.47 (23–74)	51.9 ± 13.4 (21–74)	0.003
LTТА (°)	89.31 ± 11.46 (59.76–142.14)	92.58 ± 6.31 (82.95–110.66)	89.42 ± 14.07 (67.75–142.14)	85.60 ± 11.90 (59.76–107.73)	0.052
Rüedi-Allgöwer					0.093 ($\chi^2 = 7.969$)
I	5	1	2	2	
II	25	12	3	10	
III	66	20	28	18	
AO-OTA					0.144 ($\chi^2 = 14.695$)
B1	1	1	0	0	
B2	4	2	1	1	
B3	13	9	3	1	
C1	1	0	1	0	
C2	6	2	1	3	
C3	71	19	27	25	
AO-OTA B_C					0.005 ($\chi^2 = 10.547$)
B	18	12	4	2	
C	78	21	29	28	
Topliss					0.089 ($\chi^2 = 4.841$)
Coronal type	43	15	11	17	
Sagittal type	53	18	22	13	
Coronal angulation					0.006 ($\chi^2 = 10.326$)
Varus (TTA > 90°)	52	25	16	11	
Valgus (TTA < 90°)	44	8	17	19	

Values are presented as mean ± standard deviation (range).

LTТА : lateral tibiotalar angle, OTA: Orthopaedic Trauma Association, TTA: tibiotalar angle.

Varus angulation and valgus angulation were observed in 52 patients (54.2%) and 44 patients (45.8%), respectively. According to fibular injury patterns, 33 patients (34.4%), 33 patients (34.4%), and 30 patients (31.3%) had intact fibula, simple fractures, and multifragment fractures, respectively. When the Hosmer–Lemeshow goodness-of-fit test was performed with the fibular injury pattern as the dependent variable, the p-value was 0.074 ($p > 0.005$). Therefore, the logistic regression model was statistically significant. Among explanatory variables, including the Rüedi–Allgöwer classification, simplified AO/OTA classification, and Topliss classification, the AO/OTA classification was the only variable with a statistically significant odds ratio of 5.583 ($p = 0.003$). Type C fractures of AO/OTA classification were also observed more frequently in the fractured fibula group than in the intact fibula group ($p = 0.005$, $\chi^2 = 10.240$). Conversely, in the Rüedi–Allgöwer classification, the fibular fractures did not affect the severity of pi-

lon fractures. Thus, it might be unreasonable to judge the severity according to classification alone.

Based on the linear regression analysis between varus/valgus angulation and fibular injury patterns, as the fibular fracture became more complex, the prevalence of pilon fractures of valgus angulation became higher ($p = 0.002$) (Fig. 4). Based on fibular injury patterns, LTTAs for the intact fibular group, the simple fracture group, and the multifragment group were 92.58° (range, 82.95°–110.66°; SD, 6.31), 89.42° (range, 67.75°–142.14°; SD, 14.07), and 85.60° (range, 59.76°–107.73°; SD, 11.90), respectively. The interobserver reliability of LTTA was 0.994 (95% confidence interval, 0.991–0.996) ($p < 0.001$). LTTA was not significantly different between the groups ($p = 0.052$) (Fig. 5). In the simplified AO/OTA classification, simple (87.9%) and multifragment (93.3%) groups more frequently had C-type fractures than the intact group (63.6%) ($p = 0.005$). Based on the Rüedi–Allgöwer classification, type III was observed more frequently in the simple group (84.8%) than in the intact group (68%) and the multifragment

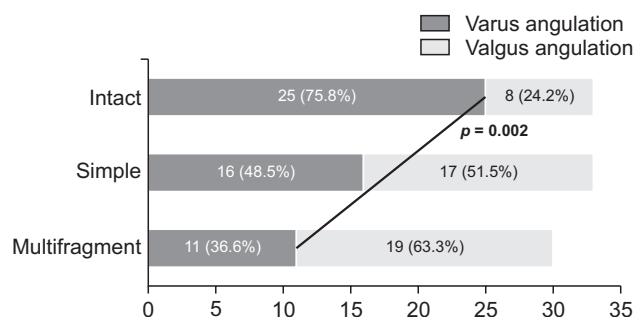


Fig. 4. Prevalence of varus or valgus angulation in each fibular injury pattern group (intact, simple, and multifragment). A linear-by-linear association test showed a significant increasing trend of valgus angulation as fibular injury patterns became more complex ($p = 0.002$).

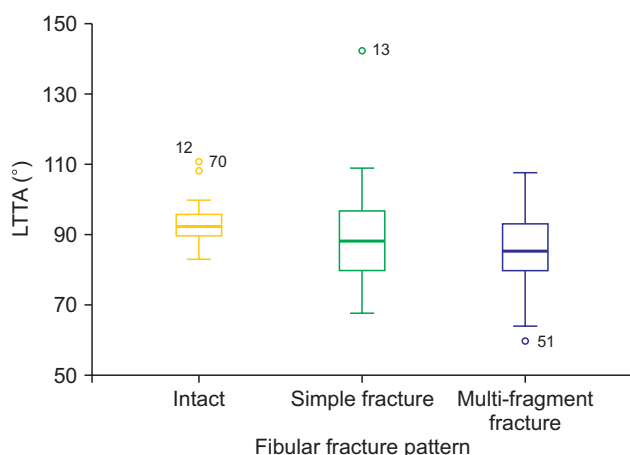


Fig. 5. Comparison of the mean lateral tibiotalar angle (LTTA) measured in each fibular injury pattern group using analysis of variance ($p = 0.052$).

Table 2. Overall Characteristics and Comparison of Pilon Fracture Based on Coronal Angulation

Variable	Total (n = 96)	Varus angulation (n = 52)	Valgus angulation (n = 44)	p-value
Rüedi–Allgöwer				0.457 ($\chi^2 = 1.565$)
I	5	4	1	
II	25	14	11	
III	66	34	32	
AO-OTA				0.197 ($\chi^2 = 7.326$)
B1	1	1	0	
B2	4	3	1	
B3	13	9	4	
C1	1	1	0	
C2	6	5	1	
C3	71	33	38	
AO-OTA B_C				0.088 ($\chi^2 = 2.909$)
B	18	13	5	
C	78	39	39	
Topliss				0.265 ($\chi^2 = 1.245$)
Coronal type	43	26	17	
Sagittal type	53	26	27	

OTA: Orthopaedic Trauma Association.

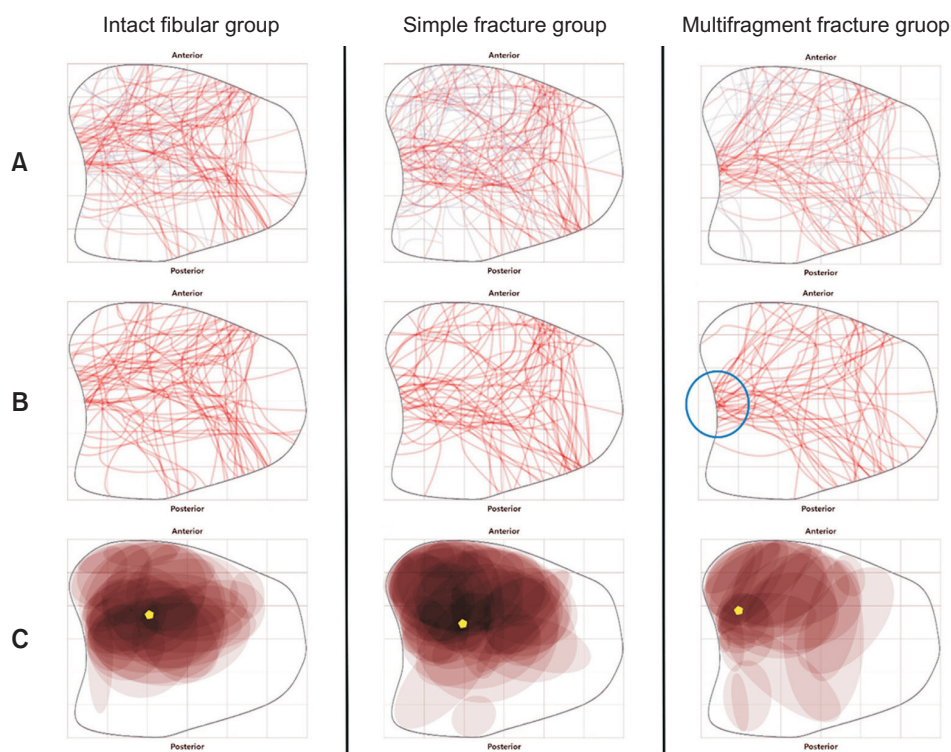


Fig. 6. Overlapped images illustrated according to the fibular injury pattern. (A) Fracture line. (B) Main fracture line. (C) Comminution zone. The blue circle shows that the main fracture line is concentrated in the incisura. The yellow pentagon marks the darkest comminution zone.

group (60.0%) ($p = 0.093$). Based on the Topliss classification, the coronal family was more frequent (56.7%) in the multifragment pattern group and the sagittal family was more frequent (66.7%) in the simple pattern group, although the difference was not statistically significant ($p = 0.089$) (Table 1). When fibular injury patterns were analyzed, the difference was only significant in the simplified AO/OTA classification. According to the varus/valgus angulation, the distribution of pilon fracture classification was not different grossly (Table 2).

Based on the plafond template of all enrolled fractures, principal fracture lines of all cases formed grossly Y corridors (Fig. 6). The thickest comminution zone was most often located in the anterolateral quadrant. According to fibular injury patterns, the comminution zone of the multifragment group was placed two grids more lateral than intact and simple fracture groups. Lateral exits of the principal fracture line in the multifragment group were much more concentrated within the fibular incisura (Fig. 6).

DISCUSSION

Correct identification of fracture characteristics, including articular involvement and metaphyseal comminution, is crucial for preoperative planning in the management of complex pilon fractures.^{1,3,4} For this purpose, CT scanning is widely used to evaluate the morphology of pilon

fractures. Past research¹⁴ revealed six distinct fragments at the articular surface by analyzing 108 articular CT scanning and provided a greater understanding of fracture morphology. Recently, the fracture mapping technique of articular comminuted fractures enabled learning of new facts of consistent fracture patterns and the locations of comminution involved.¹⁵ To the best of our knowledge, a clinical CT-based mapping study of pilon fractures according to fibular injury patterns has not been reported yet. Therefore, we commenced the present mapping study using CT scanning images of all pilon fractures caused by high-energy injury. We had several interesting findings: (1) there was no significant difference in LTTA (varus/valgus angulation) based on fibular injury patterns; (2) the severest comminution zones of the intact and simple fracture groups were placed two grids more central than those of the multifragment fracture group; and (3) in the AO/OTA classification, simple and multifragment groups of fibular injury patterns more frequently had C-type fractures than did the intact group.

Concerning that fibular injury patterns could be used to estimate the severity of injury, Barei et al.¹⁷ suggested two contradictory theories. Our radiographic analysis confirmed that pilon fractures were more severe in the fractured fibula group than in the intact fibula group. A similar result has been reported in other studies such as the study of Luk et al.¹⁸ Among explanatory variables,

including the Rüedi-Allgöwer classification, simplified AO/OTA classification, and Topliss classification, the AO/OTA classification was the only variable with a statistically significant odds ratio of 5.583 ($p = 0.003$). Type C fractures of AO/OTA classification were also observed more frequently in the fractured fibula group than in the intact fibula group ($p = 0.005$, $\chi^2 = 10.240$). Conversely, in the Rüedi-Allgöwer classification, the fibular fractures did not affect the severity of pilon fractures. Thus, it might be unreasonable to judge the severity according to classification alone.

Typically, deciding which fixation is biomechanically optimal clinically undergoes a careful analysis of the fibula fracture due to tension or compression failure. Concerning that tension/compression failures of the fibula are very closely related to the coronal alignment of the talus (LTTA), coronal angulation of the ankle at the initial radiograph has been used to discriminate the injury force and fracture patterns. However, based on our results, the LTTA was not significantly different between the groups of fibular injury patterns ($p = 0.052$). Generally, most patients were splinted before arriving the hospital. Thus, a simple reduction was attempted in the field at the scene of injury. To anticipate a biomechanically optimal site for definitive plate fixation, fibular injury patterns of intact, simple, and multifragment type might be practically more useful than the variable of LTTA without additional procedure before CT scanning.

In particular, to identify the pattern of intra-articular fractures, CT axial images of 3 mm in thickness are

mostly used.^{15,19,20} However, based on clinical experiences, it is difficult to estimate the articular fracture pattern by axial scanning images for pilon fractures with severe displacement. It has long been recognized that the fracture assessment is dependent on the nature of cut chosen for impacted fragments (die-punch fragment) (Fig. 7). Thus, some studies^{21,22} have attempted to mount images and perform a hypothetical reduction using the Mimics software as a specialized equipment/software. Recently, the fracture mapping technique has been used in several studies^{4,15,19-23} to identify a consistent fracture pattern by diagrammatizing the fracture line and comminution zone. Cole et al.¹⁵ have confirmed that the comminution zone most commonly exists on the anterolateral side and that the principal fracture line forms the Y-corridor by performing pilon fracture mapping. Although they targeted only the C3 type of AO/OTA classification, all types of pilon fractures were enrolled in the present study. Based on our results, the comminution zone of multifragment group was located two grids more lateral than that in the intact and simple fracture groups. Furthermore, the principal line and comminution zone were concentrated in the fibular incisura. In the multi-fragment group, the injury force might be applied to the lateral (incisura) area owing to valgus stress (Fig. 8). Luk et al.¹⁸ have divided the plafond into seven sections to confirm the difference in the comminution zone between the intact fibula group and the fractured fibula group. They could not confirm a statistical difference between the two groups.¹⁸ However, our study demonstrated that in the intact and simple fracture groups, the comminuted zone was placed two grids more central than

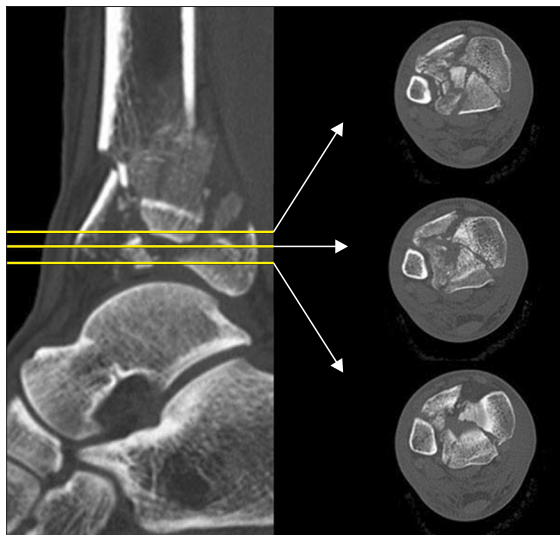


Fig. 7. It is difficult to determine the articular surface if there is an impacted fragment (die-punch fragment). Even a little change in the level of the articular surface results in a difference in the computed tomography axial cut image.

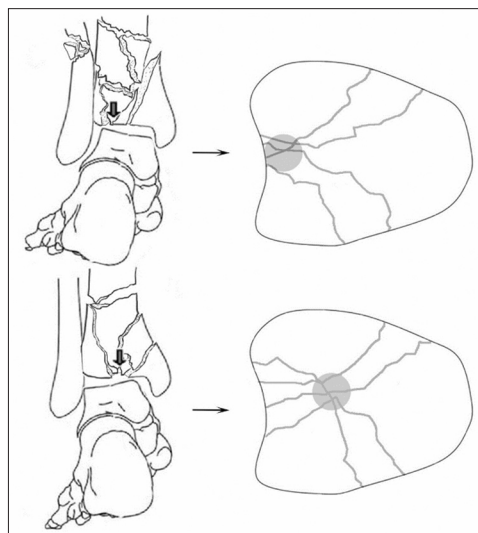


Fig. 8. Simplified diagrams of fibular injury patterns and tibial plafond fracture patterns according to varus or valgus force.

that in the multifragment group. Although the severity of the articular surface injury cannot be determined,^{3,24)} our information on the comminution zone according to fibular injury patterns could be utilized for determining a preoperative strategy of plate fixation, medial vs. anterolateral plate fixation. Based on Busel et al.'s assertion⁵⁾ that the fibular injury pattern can be an influencing factor in deciding the location of definitive plate fixation, our results might be applied clinically for repairing metaphyseal length and stability.^{5,9)} Recently, a few studies have demonstrated that there exists a difference in the severity of pilon fractures according to fibular fractures^{17,18)} and fracture patterns, which allows us to estimate the injury mechanism.^{5,8,9)} Concerning this issue, we found that simple (87.9%) and multifragment (93.3%) groups more frequently had C-type fractures of AO/OTA classification than did the intact group (63.6%).

However, our radiographic analysis has several fundamental limitations. Firstly, many factors that could influence fractures were not considered. Complex injury mechanisms including turning force and anteroposterior shearing force cannot be described with pressure. Secondly, patients' underlying medical issues influencing bone metabolism were not inspected. Thirdly, there was no method to statistically compare the diagrammatized fracture map. Fourthly, there were inaccuracies in classification because CT scans before external fixation were included. Despite these limitations, our findings are valuable

for understanding the comminuted zone of pilon fractures based on fibular injury patterns. These findings could help determine the preoperative strategy including an optimal approach and definitive plate fixation.

Compared with that of the intact and simple fracture groups, the comminution zone of the multifragment group was located two grids more lateral and the principal line was concentrated in the incisura. Considering fibular injury patterns of pilon fractures, preoperative strategies for surgical approaches and definitive fixation methods could be guided by anticipating the comminution zone and the principal fracture line.

CONFLICT OF INTEREST

No potential conflict of interest relevant to this article was reported.

ORCID

Jae-Hwan Lim	https://orcid.org/0000-0001-7043-1568
Jun-Young Lee	https://orcid.org/0000-0002-9764-339X
Ba-Rom Kim	https://orcid.org/0000-0001-5341-1717
Suenghwan Jo	https://orcid.org/0000-0002-3378-5954
Dong-Hyuk Cha	https://orcid.org/0000-0001-8159-1567
Hyo-Jun Lee	https://orcid.org/0000-0001-5091-6154
Gu-Hee Jung	https://orcid.org/0000-0002-9751-4678

REFERENCES

1. Tornetta P III, Ricci WM, Ostrum RF, McQueen MM, McKee MD, Court-Brown CM. Rockwood and Green's fractures in adults. Lippincott Williams & Wilkins; 2019.
2. Liporace FA, Yoon RS. Decisions and staging leading to definitive open management of pilon fractures: where have we come from and where are we now? *J Orthop Trauma*. 2012; 26(8):488-98.
3. Penny P, Swords M, Heisler J, Cien A, Sands A, Cole P. Ability of modern distal tibia plates to stabilize comminuted pilon fracture fragments: is dual plate fixation necessary? *Injury*. 2016;47(8):1761-9.
4. Tornetta P, Gorup J. Axial computed tomography of pilon fractures. *Clin Orthop Relat Res*. 1996;(323):273-6.
5. Busel GA, Watson JT, Israel H. Evaluation of fibular fracture type vs location of tibial fixation of pilon fractures. *Foot Ankle Int*. 2017;38(6):650-5.
6. Egol KA, Wolinsky P, Koval KJ. Open reduction and internal fixation of tibial pilon fractures. *Foot Ankle Clin*. 2000; 5(4):873-85.
7. Lee YS, Chen SW, Chen SH, Chen WC, Lau MJ, Hsu TL. Stabilisation of the fractured fibula plays an important role in the treatment of pilon fractures: a retrospective comparison of fibular fixation methods. *Int Orthop*. 2009;33(3):695-9.
8. Sirkin MS. Plating of tibial pilon fractures. *Am J Orthop (Belle Mead NJ)*. 2007;36(12 Suppl 2):13-7.
9. Busel GA, Watson JT. Plating of pilon fractures based on the orientation of the fibular shaft component: a biomechanical study evaluating plate stiffness in a cadaveric fracture model. *J Orthop*. 2017;14(2):308-12.
10. Gustilo RB, Anderson JT. Prevention of infection in the treatment of one thousand and twenty-five open fractures of long bones: retrospective and prospective analyses. *J Bone Joint Surg Am*. 1976;58(4):453-8.
11. Najefi AA, Buraimoh O, Blackwell J, et al. Should the tibio-

- talar angle be measured using an AP or mortise radiograph? Does it matter? *J Foot Ankle Surg.* 2019;58(5):930-2.
12. Rüedi TP, Allgower M. The operative treatment of intra-articular fractures of the lower end of the tibia. *Clin Orthop Relat Res.* 1979;(138):105-10.
 13. Muller ME, Nazarian S, Koch P, Schatzker J. The comprehensive classification of fractures of long bones. Springer Science & Business Media; 2012.
 14. Topliss CJ, Jackson M, Atkins RM. Anatomy of pilon fractures of the distal tibia. *J Bone Joint Surg Br.* 2005;87(5):692-7.
 15. Cole PA, Mehrle RK, Bhandari M, Zlowodzki M. The pilon map: fracture lines and comminution zones in OTA/AO type 43C3 pilon fractures. *J Orthop Trauma.* 2013;27(7):e152-6.
 16. McGonagle L, Cordier T, Link BC, Rickman MS, Solomon LB. Tibia plateau fracture mapping and its influence on fracture fixation. *J Orthop Traumatol.* 2019;20(1):12.
 17. Barei DP, Nork SE, Bellabarba C, Sangeorzan BJ. Is the absence of an ipsilateral fibular fracture predictive of increased radiographic tibial pilon fracture severity? *J Orthop Trauma.* 2006;20(1):6-10.
 18. Luk PC, Charlton TP, Lee J, Thordarson DB. Ipsilateral intact fibula as a predictor of tibial plafond fracture pattern and severity. *Foot Ankle Int.* 2013;34(10):1421-6.
 19. Hendrickx LA, Cain ME, Sierevelt IN, et al. Incidence, predictors, and fracture mapping of (Occult) posterior malleolar fractures associated with tibial shaft fractures. *J Orthop Trauma.* 2019;33(12):e452-8.
 20. Misir A, Ozturk K, Kizkapan TB, Yildiz KI, Gur V, Sevensan A. Fracture lines and comminution zones in OTA/AO type 23C3 distal radius fractures: the distal radius map. *J Orthop Surg (Hong Kong).* 2018;26(1):2309499017754107.
 21. Xie X, Zhan Y, Dong M, et al. Two and three-dimensional CT mapping of Hoffa fractures. *J Bone Joint Surg Am.* 2017;99(21):1866-74.
 22. Zhang X, Zhang Y, Fan J, Yuan F, Tang Q, Xian CJ. Analyses of fracture line distribution in intra-articular distal radius fractures. *Radiol Med.* 2019;124(7):613-9.
 23. Armitage BM, Wijdicks CA, Tarkin IS, et al. Mapping of scapular fractures with three-dimensional computed tomography. *J Bone Joint Surg Am.* 2009;91(9):2222-8.
 24. Beardsley C, Marsh JL, Brown T. Quantifying comminution as a measurement of severity of articular injury. *Clin Orthop Relat Res.* 2004;(423):74-8.